Superconductivity in ropes of carbon nanotubes

M. Ferrier[1], A. De Martino[2,*], A. Kasumov[1,3,†],
S. Guéron[1], M. Kociak [1], R. Egger[2] and H. Bouchiat[1]
[1]*Laboratoire de Physique des Solides, Associé au CNRS,*
Bâtiment 510, Université Paris-Sud, F-91405 Orsay, France
[2]*Institut für Theoretische Physik, Heinrich-*
Heine-Universität, D-40225 Düsseldorf, Germany
[3]*Institute of Microelectronics Technology and High Purity Materials,*
Russian Academy of Sciences, Chernogolovka 142432 Moscow Region, Russia

Abstract

Recent experimental and theoretical results on intrinsic superconductivity in ropes of single-wall carbon nanotubes are reviewed and compared. We find strong experimental evidence for superconductivity when the distance between the normal electrodes is large enough. This indicates the presence of attractive phonon-mediated interactions in carbon nanotubes, which can even overcome the repulsive Coulomb interactions. The effective low-energy theory of rope superconductivity explains the experimental results on the temperature-dependent resistance below the transition temperature in terms of quantum phase slips. Quantitative agreement with only one fit parameter can be obtained. Nanotube ropes thus represent superconductors in an extreme 1D limit never explored before.

KEYWORDS: A. Nanostructures, Superconductors; D. Electron transport, Phase transitions

PACS numbers: 74.70.-b, 74.78.Na, 74.25.Fy

* Corresponding author. Address: Institut für Theoretische Physik, Heinrich-Heine-Universität, Universitätsstraße 1, Gebäude 25.32, D-40225 Düsseldorf, Germany; E-mail: ademarti@thphy.uni-duesseldorf.de
† Present address: RIKEN, Hirosawa 2-1, Wako, Saitama, 351-0198 Japan

I. INTRODUCTION

The hope to use molecules as the ultimate elementary building blocks for electronic circuits has motivated the quest to understand electronic transport in thinner and thinner wires, ideally with one or two conduction modes. However, a number of physical phenomena tend to drive one-dimensional (1D) metallic wires to an insulating state at low temperature. Carbon nanotubes, because of their special band structure, can escape such a fate and remain conducting over lengths greater than one micron down to very low temperature [1, 2]. Moreover, transport through nanotubes has been shown to be quantum coherent [3]. This is also demonstrated by the existence of strong supercurrents when individual nanotubes are connected to superconducting contacts [4, 5]. The observation of *intrinsic superconductivity* in ropes of carbon nanotubes containing a few tens of tubes [6, 7] is even more surprising and indicates the presence of attractive pairing interactions which overcome the strong repulsive interactions. This phenomenon is described in the present paper, both from the experimental and the theoretical point of view. A single-wall nanotube (SWNT) is made of a single graphene plane wrapped into a cylinder. The Fermi surface of graphene reduces to two discrete points (usually denoted as K and K') at the corners of the first Brillouin zone [8]. As a result, depending on the diameter and helicity, which determine the boundary conditions of the electronic wave functions around the tube, a SWNT can be either semiconducting or metallic [1, 2]. A metallic SWNT is characterized by just two conduction channels, low electronic density, Fermi velocity v_F nearly as high as in copper, and long mean free path [9]. These properties make them long sought-after realizations of 1D conductors. In one dimension, repulsive electron-electron interactions lead to an exotic correlated electronic state, the Luttinger liquid (LL) [10, 11]. In a LL, collective plasmon-like excitations give rise to anomalies in the single-particle density of states, and long-range order cannot survive even at zero temperature. The low-energy theory of SWNTs [12, 13] predicts a metallic SWNT to constitute a realization of a four-channel LL, with channel index $a = c+, c-, s+, s-$ corresponding to total/relative charge/spin degrees of freedom. These arise due to the $K - K'$ degeneracy and the electronic spin. The interaction strength in a SWNT is then parameterized by a single dimensionless parameter g, where $g = 1$ in the absence of interactions. For repulsive Coulomb interactions, this parameter is smaller than unity, with concrete estimates for SWNTs in the range $g \approx 0.2$ to 0.3 [12, 13]. For attractive

interactions caused by phonon exchange, as long as retardation effects are negligible, one instead obtains a LL with $g > 1$. In general, both effects have to be combined on equal footing. For superconductivity to occur, it appears to be necessary to have effectively $g > 1$.

Experimental evidence for the validity of LL theory in a SWNT has been provided by measurements of the tunneling resistance diverging as a power law with temperature [14, 15], from photoemission spectroscopy [16], and from transport properties of crossed SWNTs [17]. From these experimental results, values for the LL parameter in the range $g \approx 0.16$ to 0.3, consistent with theoretical expectations, were extracted. Such small values for g correspond to pronounced repulsive interactions, and would imply that at very low temperature an insulating state is reached unless the material is extremely clean. The measurements in Refs. [14, 15, 17] were done on individual nanotubes connected to the measuring leads through tunnel junctions. Because of the onset of Coulomb blockade [18], the low-temperature small-voltage regime has not been explored in depth. We have developed a technique in which measuring pads are connected through low-resistance contacts to *suspended* nanotubes [19]. Ropes and individual SWNTs connected to normal contacts using this technique exhibit only very weak temperature and bias dependence of the resistance down to 1K. More surprisingly, we have reported experimental evidence of intrinsic superconductivity below 0.5 K in ropes, provided that the distance between the normal electrodes is large enough [6, 7]. In this paper, we discuss the 1D character of the transition and the physical parameters that govern this transition, such as the length of the rope, the number of metallic SWNTs in the rope, the intertube couplings, disorder, and so on. Below we summarize both our experimental results [6, 7] and the low-energy theory describing the superconducting state in ropes proposed by two of us [20, 21]. Fortunately, the measured low-temperature data for the resistance allow to perform detailed tests of the theory. In this theory, the rope is modelled as an array of N metallic SWNTs with effectively attractive intratube interactions, coupled together by Cooper-pair hopping. Attractive phonon-mediated interactions may overcome the Coulomb repulsion in a sufficiently thick rope, leading to a LL parameter $g > 1$. The dominant 1D fluctuations on individual SWNTs then cause the incipient formation of singlet Cooper pairs. Superconductivity of the rope is finally stabilized by Cooper pair hopping between the tubes (Josephson coupling), see also Refs. [22, 23, 24]. Since typical elastic mean free paths in metallic SWNTs may exceed 1 μm [1, 9], intratube disorder is completely neglected. However, disorder due to the random distribution of tube

chiralities in the rope, where only 1/3 of the SWNTs is expected to be metallic [1, 2], is taken into account in the following way. First, due to momentum-conservation arguments, it strongly suppresses single-particle hopping between adjacent SWNTs [22, 25], which is thus neglected henceforth. Second, we introduce a matrix Λ, whose elements Λ_{ij} represent the Josephson couplings between the ith and the jth tube, where $i, j = 1, \ldots, N$. In order to simulate the random distribution of tube chiralities, Λ should be drawn from an appropriate random distribution. Typically, $\Lambda_{ij} \approx a_0 t_\perp^2 / \Delta E$ when metallic tubes are nearest neighbors, and zero otherwise. Here, $a_0 = 0.24$ nm is the lattice spacing, $t_\perp$ is the transverse intertube hopping energy, and ΔE is the typical energy band spacing within one tube [23]. However, detailed information about Λ is not needed in the low-energy regime, and general results can be derived for a fixed but unspecified Λ. For this model, the effective action for the proper order parameter allows to identify a mean-field transition temperature T_c^0. For $T < T_c^0$, the amplitude of the order parameter is finite, but due to the reduced dimensionality, phase fluctuations may still destroy superconductivity [26]. Such fluctuations are shown to indeed cause a depression of the true transition temperature T_c below the mean-field value, which can be linked to the proliferation of quantum phase slips (QPSs). A QPS is a topological vortex-like excitation of the superconducting phase field, which only exists in 1D superconductors [26]. In addition to the T_c depression, QPSs produce a finite sub-T_c linear resistance apart from the usual temperature-independent contact resistance. This effect is indeed observed experimentally, and can be compared in a quantitative way to theory. Our theory makes detailed predictions about the temperature dependence of this resistance, where almost all free parameters can be determined independently. There is essentially only one free (dimensionless) fit parameter, which should have a value close to unity. This turns indeed out to be the case.

This paper is organized as follows. In Sec. II, we summarize and discuss experimental results on intrinsic superconductivity in ropes of carbon nanotubes. In Sec. III, the effective low-energy theory of rope superconductivity is reviewed. In Sec. IV, the theoretical predictions are compared with the experimental results. The rather good agreement found there supports the notion that ropes represent 1D superconductors in the few-channel limit, where QPSs can be experimentally observed in a clear manner from the temperature-dependent resistance below T_c.

II. EXPERIMENTAL EVIDENCE FOR ROPE SUPERCONDUCTIVITY

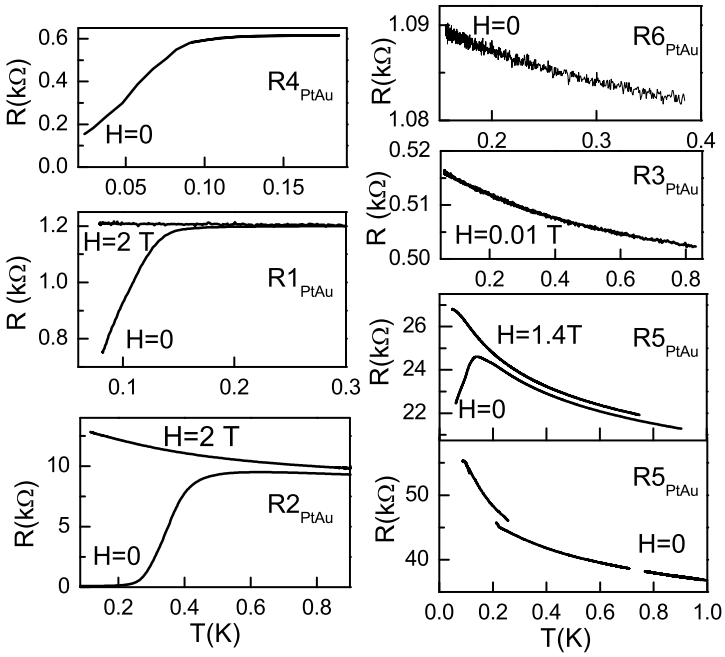

FIG. 1: Resistance as a function of temperature for the six samples described in Table I, both for zero and large magnetic fields.

In this section, we review experimental results from Ref. [7] reporting evidence for intrinsic superconductivity in ropes of carbon nanotubes. We start with a discussion of the low-temperature (below 1 K) transport regime of suspended ropes of SWNTs connected to

	L	N	R_{290K}	$R_{4.2K}$	T*	I_c	$I_c{}^*$
$R1_{PtAu}$	2 μm	350	10.5 $k\Omega$	1.2 $k\Omega$	140 mK	0.1 μA	0.36 μA
$R2_{PtAu}$	1 μm	350	4.2$k\Omega$	9.2$k\Omega$	550 mK	0.075 μA	3 μA
$R3_{PtAu}$	0.3μm	350	400 Ω	450 Ω	*	*	*
$R4_{PtAu}$	1μm	45	620 Ω	620 Ω	120 mK	*	0.1 μA
$R5_{PtAu}$	2 μm	300	16 $k\Omega$	21 $k\Omega$	130 mK	20 nA	0.12 μA
$R6_{PtAu}$	0.3 μm	200	240 Ω	240 Ω	*	*	*

TABLE I: Summary of the characteristics of six ropes mounted on Pt/Au contacts. T^* is the transition temperature below which the resistance starts to drop, I_c is the current at which the first resistance increase occurs, and I_c^* is the current at which the last resistance jump occurs.

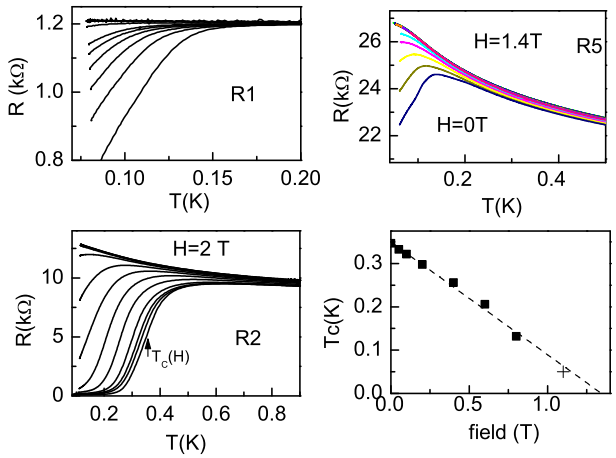

FIG. 2: Resistance as a function of temperature for samples $R1, 2, 5_{PtAu}$ showing a transition. The resistance of $R1$ is measured in magnetic fields of $\mu_0 H$= 0, 0.02, 0.04, 0.06, 0.08, 0.1, 0.2, 0.4, 0.6, 0.8 and 1 T from bottom to top. The resistance of $R2$ is taken at $\mu_0 H$=0, 0.05, 0.1, 0.2, 0.4, 0.6, 0.8, 1, 1.25, 1.5, 1.75, 2, 2.5 T (from bottom to top), that of $R5$ at $\mu_0 H$=0, 0.1, 0.2, 0.3, 0.5, 1.4 T (from bottom to top). Bottom right: $T_c(H)$ for $R2$.

normal electrodes. The electrodes are trilayers of sputtered $Al_2O_3/Pt/Au$ of respective thickness 5, 3 and 200 nm. They do not show any sign of superconductivity down to 50 mK. As is shown in Fig. 1, different behaviors are observed for the temperature dependence of the linear resistance. The resistance of short samples whose length is of the order of 0.3 μm ($R3_{PtAu}$ and $R6_{PtAu}$) increases weakly and monotonously as temperature is reduced, whereas the resistance of samples longer than 1 μm ($R1, 2, 4, 5_{PtAu}$) drops over a relatively broad temperature range, starting below a transition temperature T^* between 0.4 and 0.1 K, see Table I. The resistance of $R1_{PtAu}$ is reduced by 30% at 70 mK, and that of $R4_{PtAu}$ by 75% at 20 mK. In both cases, no inflection point in the temperature dependence is observed. On the other hand, the resistance of $R2_{PtAu}$ decreases by more than two orders of magnitude, and reaches a constant value below 100 mK, namely $R_r = 74\ \Omega$. This residual resistance R_r is interpreted as a contact resistance which must be present even in the superconducting phase. The contact resistance arises because only a finite number N of metallic SWNTs is coupled to the normal-conducting pads. Since each metallic SWNT has two spin-degenerate conduction channels,

$$R_r = R_Q/2N, \quad R_Q = h/2e^2 = 12.9\ \mathrm{k}\Omega. \tag{1}$$

Since the residual resistance can be experimentally determined quite accurately, at least for the two samples $R2$ and $R4$, the number N can be obtained directly using Eq. (1). This number is an important parameter for the theory described in Sec. III.

The low-temperature drop of the resistance below T^* disappears when increasing the magnetic field. For all samples, a critical field can be defined, above which the normal-state resistance is recovered. As shown in Fig. 2, this critical field decreases linearly with temperature, very similar to what is seen in SWNTs and ropes connected to superconducting contacts [4, 5]. We define a critical field H_c as the extrapolation of $H_c(T)$ to zero temperature, see Fig. 2. Above the critical field, the resistance increases with decreasing temperature, similar to ropes $R3$ and $R6$, and becomes independent of magnetic field. Figures 3 and 4 show that in the temperature and field range where the linear resistance drops, the differential resistance is strongly current-dependent, with lower resistance at low current. These data suggest that the ropes $R1, R2$, and $R4$ are superconducting. Although the experimental curves for $R2_{PtAu}$ look similar to those of SWNTs connected to superconducting contacts [4], there are major differences. In particular the $V(I)$ and $dV/dI(I)$ curves found here do not show any supercurrent because the contacts are normal metals, implying a finite residual resistance.

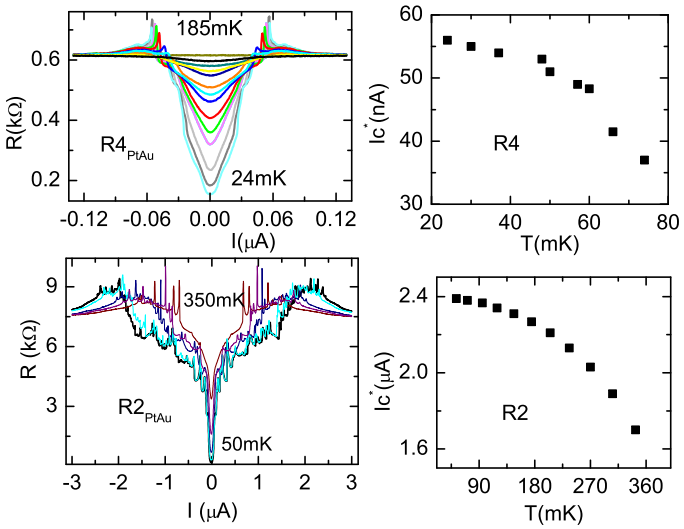

FIG. 3: Differential resistance of $R2_{PtAu}$ and $R4_{PtAu}$ at different temperatures. Right panel: Temperature dependence of I_c^*, the current at which the last resistance jumps occur in the dV/dI curves.

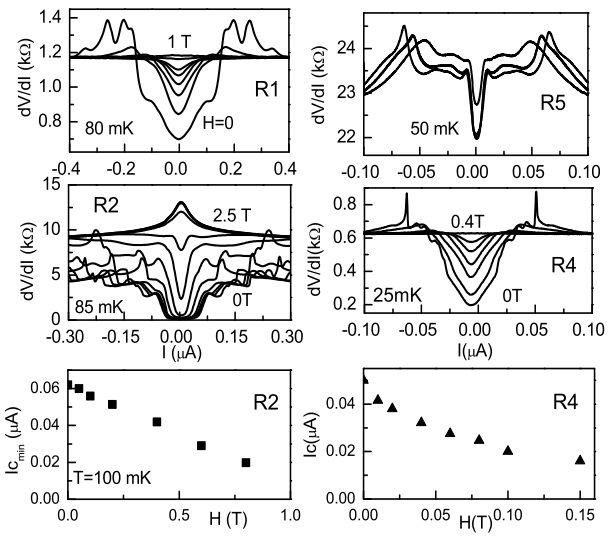

FIG. 4: Differential resistance as a function of current for samples $R1,2,4,5_{PtAu}$ in different applied fields. Sample $R1$: Fields are 0, 0.02, 0.04, 0.06, 0.08, 0.1, 0.2 and 1 T. Sample $R2$: Fields are 0, 0.2, 0.4, 0.6, 0.8, 1, 1.25, 1.5, 1.75, 2, and 2.5 T. Sample $R5$: Fields are 0.02, 0.04, 0.06, 0.08 T. Sample $R4$: Fields are 0, 0.02, 0.06, 0.1, 0.15, 0.2 and 0.4 T. Bottom: Field dependence of I_c for samples $R2_{PtAu}$ and $R4_{PtAu}$. Note the linear behavior.

The observed jumps in the differential resistance as the current is increased, see Fig. 5, are similar to the behavior observed in long narrow superconducting metal wires in the very vicinity of the transition temperature. However, in the present case these jumps are observed down to very low temperature [27]. For sample $R2$, the differential resistance at low current remains equal to R_r up to 50 nA, where it strongly rises but does not recover its normal-state value until 2.5 μA. The jump in resistance at the first step corresponds approximately to the normal-state resistance of a length ξ of sample $R2$ (R_ξ), where ξ is the superconducting coherence length estimated from $\xi = \sqrt{\hbar D/\Delta}$ where Δ is the BCS gap related to the transition temperature T^* and D the diffusion constant describing transport in the rope in the normal state. Each peak corresponds to a hysteretic feature in the $V - I$ curve, see Fig. 5. These jumps are identified as phase slips [26, 27, 28], which reflect the occurrence of normal regions located around defects in the sample. Such phase slips could be thermally activated phase slips (TAPSs), leading to a roughly exponential decrease of the resistance instead of a sharp transition. At sufficiently low temperature and voltage, instead of the TAPSs, quantum phase slips (QPSs) of typical size ξ are expected to dominate. The

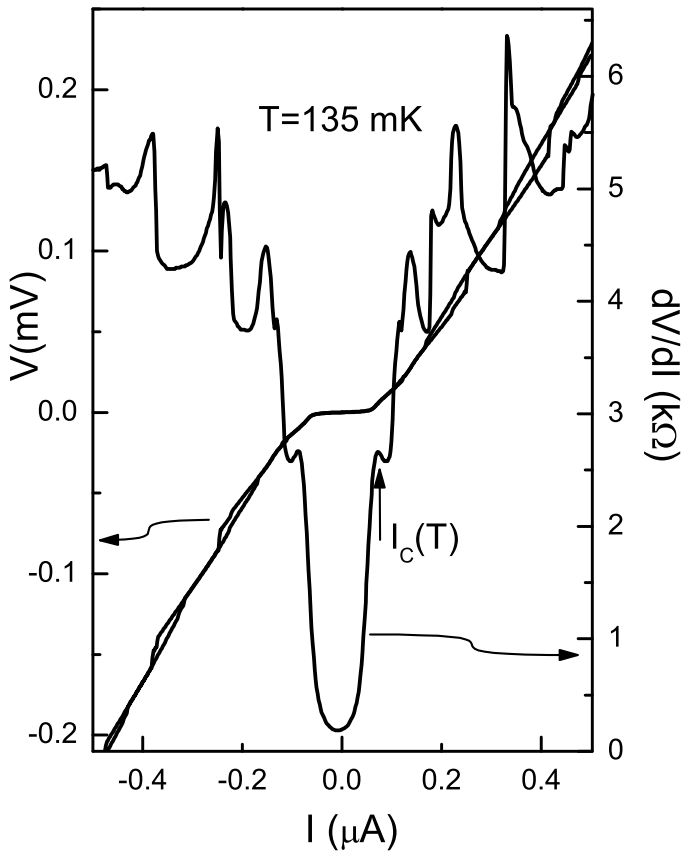

FIG. 5: $V(I)$ and $dV/dI(I)$ curves for sample $R2_{PtAu}$. Note the hysteretic behavior in $V(I)$ at each peak in the $\frac{dV}{dI}(I)$ curve.

competition between TAPS and QPS processes is addressed briefly in Sec. III below. In sample $R2$, the current at which the first resistance jump occurs (60 nA, see Fig. 4) is close to the critical current expected theoretically for a diffusive superconducting wire [29],

$$I_c = \Delta_2/eR_\xi \approx 20 \text{ nA},$$

with gap $\Delta_2 = 85$ μeV. On the other hand, the current at which the last resistance jump occurs (2.4 μA, see Fig. 3) is close to the critical current of a ballistic superconducting wire with the same number of conducting channels [26],

$$I_c^* = \frac{\Delta_2}{eR_r} \approx 1 \ \mu\text{A}.$$

Before analyzing the data further, we wish to emphasize that this is the first observation of superconductivity in wires with $N < 100$ conduction channels. Earlier experiments in

nanowires [27, 30, 31] dealt with at least a few thousand channels. We therefore expect a strong 1D behavior for the transition. In particular, the broadness of the resistance drop with temperature is linked to large fluctuations of the superconducting order parameter as expected in one dimension. An important parameter is the number of tubes in the rope. If there are only a few tubes in the rope, the system is very close to the strict 1D limit, and the transition is very broad. Comparing the two ropes in Fig. 6, it is clear that the transition, both in temperature and magnetic field, is much broader in sample $R4_{PtAu}$ with only ≈ 45 tubes than in $R2_{PtAu}$ with ≈ 350 tubes. Moreover, there is no inflection point in the temperature dependence of the resistance in the thinner rope, typical of a strictly 1D behavior. We also expect a stronger screening of the repulsive Coulomb interactions in the thick rope, which is also in favor of superconductivity. In the following, when comparing to theoretical predictions, we will have to take into account several essential features, e.g., the influence of the normal contacts, the finite length of the samples compared to relevant mesoscopic and superconducting scales, the effects of disorder, and the role of intertube couplings.

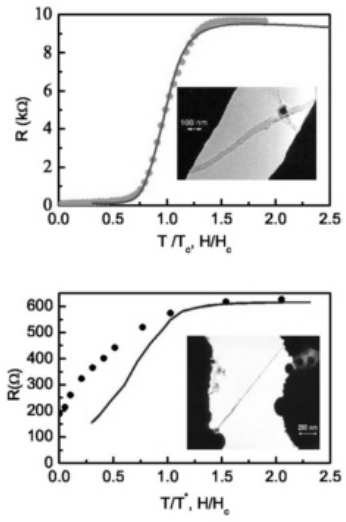

FIG. 6: Resistance as a function of temperature (continuous line) and magnetic field (scatter points) for samples $R2_{PtAu}$ and $R4_{PtAu}$. Insets: TEM micrographs of the samples.

III. EFFECTIVE LOW-ENERGY THEORY OF ROPE SUPERCONDUCTIVITY

In this section we summarize the main features of the recently proposed effective low-energy theory of intrinsic superconductivity in carbon nanotube ropes. For technical details, we refer the reader to the original publication [21]. The basic ingredients of the model have been discussed in the Introduction, see also Refs. [22, 23, 24, 25]. Within the standard bosonization approach [11], the model is described by the Euclidean action

$$S = \sum_{j=1}^{N} S_{\rm LL}^{(j)} - \sum_{jk} \Lambda_{jk} \int dx d\tau \, \mathcal{O}_j^* \mathcal{O}_k, \tag{2}$$

where $-L/2 < x < L/2$ is the spatial 1D coordinate along the individual SWNTs for rope length L, and $0 \leq \tau < 1/T$ is imaginary time (we put $\hbar = k_B = 1$ in intermediate steps). The first term describes the metallic tubes in the rope as N uncoupled identical four-channel Luttinger liquids [12, 13, 20],

$$S_{\rm LL} = \int dx d\tau \sum_{a=c\pm,s\pm} \frac{v_a}{2g_a} \left[(\partial_\tau \varphi_a / v_a)^2 + (\partial_x \varphi_a)^2 \right]. \tag{3}$$

Here the boson fields $\varphi_a(x,\tau)$ (and associated dual fields θ_a) describe the collective total/relative charge/spin plasmon-like excitations. The interaction parameter for the total charge mode $g_{c+} \equiv g$ is determined by the combined effect of Coulomb repulsion and phonon-mediated attractive interactions. If Coulomb interactions are screened off, e.g., by the other SWNTs in a thick rope [24], effectively attractive interactions are possible. In what follows, we assume $g > 1$, where $g \approx 1.3$ has been estimated for (10,10) SWNTs with good screening [20]. The interaction parameters in the neutral channels are practically not affected by interactions, $g_{c-,s+,s-} = 1$. The velocities v_a in Eq. (3) are given by $v_a = v_F/g_a$, where $v_F = 8 \times 10^5$ m/sec is the Fermi velocity. The second term in Eq. (2) describes the intertube couplings in the form of Cooper-pair hopping. The combined effects of random tube chiralities and attractive electron-electron interactions drive the incipient formation of singlet Cooper pairs on individual SWNTs. The Cooper pair operator $\mathcal{O}$ in Eq. (2) is in bosonized language expressed as [32]

$$\mathcal{O} = \frac{1}{\pi a_0} \cos[\sqrt{\pi}\theta_{c+}] \cos[\sqrt{\pi}\varphi_{c-}] \cos[\sqrt{\pi}\varphi_{s+}] \cos[\sqrt{\pi}\theta_{s-}] - (\cos \leftrightarrow \sin), \tag{4}$$

where we identify the UV cutoff necessary in the bosonization scheme with the lattice constant a_0. In order to investigate the physical properties of the system described by the action

(2), approximations are necessary. Since in 1D systems fluctuations are strong, we can expect that the order parameter amplitude remains small over a wide temperature range, and a Ginzburg-Landau-type expansion should be accurate. To that end, we first decouple the Josephson terms in Eq. (2) by performing a Hubbard-Stratonovich transformation [33]. This introduces a complex field $\Delta_i(x,\tau)$, which acts as the superconducting order parameter. The partition function for the original system can then be expressed as a functional integral over the fields Δ_i, with an effective action formally defined as a functional integral over the LL boson fields. The latter functional integral cannot be performed analytically, and one has to resort to approximate methods. A systematic approach proceeds via cumulant expansion, where the small expansion parameter is $|\Delta|/2\pi T$, and one has to keep terms (at least) up to quartic order [33]. After perfoming a gradient expansion, justified for slow temporal and spatial variations of the order parameter, i.e., in the low-energy long-wavelength regime of primary interest here, one finally obtains a quantum Ginzburg-Landau (GL) action,

$$S = \int dx d\tau \left\{ \sum_{j=1}^{N} \left[\left(\Lambda_1^{-1} - A \right) |\Delta_j|^2 + B|\Delta_j|^4 \right] + C|\partial_x \Delta_j|^2 + D|\partial_\tau \Delta_j|^2 + \sum_{jk} \Delta_j^* V_{jk} \Delta_k \right\}, \tag{5}$$

with positive temperature-dependent coefficients A, B, C, D and a real symmetric positive-definite matrix V_{ij} defined in terms of the Josephson matrix Λ, see Ref. [21] for details. Furthermore, Λ_1 is the largest eigenvalue of Λ. The GL coefficients can be computed analytically from this expansion, and are expressed in terms of the microscopic model parameters [21]. Note that we keep the imaginary-time dependence of $\Delta_i(x,\tau)$, which is essential for what follows. Thereby quantum fluctuations are fully accounted for, in contrast to standard static GL theory [26]. The coefficient $A(T)$ is found to grow as T decreases, and hence a mean-field critical temperature follows from the condition $A(T_c^0) = \Lambda_1^{-1}$. The result is

$$T_c^0 = c_0 \frac{\hbar v_F}{k_B a_0} (\Lambda_1 / \hbar v_F)^{2g/(g-1)}, \tag{6}$$

with c_0 a dimensionless prefactor of order unity. T_c^0 exhibits a dependence on N and the connectivity of the Josephson matrix through the eigenvalue Λ_1. For large N, $\Lambda_1(N)$ saturates, and Eq. (6) approaches the bulk transition temperature. Using Λ_1 estimates from Ref. [23] and typical N from Table I, we find $T_c^0 \approx 0.1$ to 1 K. A precise estimate is difficult to give because the Josephson matrix is in general unknown, and due to the typically large exponent in Eq. (6), T_c^0 depends very sensitively on Λ_1. For $T < T_c^0$, it is convenient to

adopt an amplitude-phase representation of the order parameter, $\Delta_j = |\Delta_j| \exp[i\phi_j]$. The amplitude of the order parameter field is then finite, with a gap for fluctuations around the mean-field value. This mean-field value can be directly calculated from the saddle-point equation for the action (5). The numerical solution to this equation shows that the GL expansion parameter $|\Delta|/2\pi T$ indeed remains small down to very low temperatures, and the use of GL theory is self-consistently justified [21]. Due to the mass gap for amplitude fluctuations, the amplitudes can then be fixed to their mean field value. Moreover, for $N < 100$, transverse fluctuations are negligible both regarding the amplitude, as follows from the numerical solution of the saddle-point equations, as well as concerning the phase, which follows from scaling dimension arguments. Therefore, one finally arrives at a standard Gaussian action governing the dynamics of the superconducting phase [26],

$$S = \frac{\mu}{2\pi} \int dx d\tau \left[c_s^{-1} (\partial_\tau \phi)^2 + c_s (\partial_x \phi)^2 \right], \tag{7}$$

where $\phi_j = \phi(x, \tau)$ is equal on all tubes. The superconductor's phase is the relevant fluctuation mode in a 1D system. Furthermore, c_s is the Mooij-Schön mode velocity [34], which here is of order v_F, and the dimensionless rigidity follows in the form

$$\mu(T) = N\nu \left[1 - (T/T_c^0)^{(g-1)/2g} \right], \tag{8}$$

where $\nu \approx 1$. Equation (8) for the temperature-dependent phase stiffness is one of the central results in Ref. [21]. The value of ν is difficult to compute in a very precise way. In particular, disorder and dissipation effects neglected in our model tend to decrease it [35, 36]. Therefore, ν is considered below as a fit parameter when comparing with experimental data. In fact, ν turns out to be essentially the only free fit parameter, where internal consistency of the theory constrains ν to be of order unity. In the 1D system described by the action (7), vortex-like topological excitations (quantum phase slips of size ξ) can destroy superconductivity and give rise to a broad resistive transition. This occurs via a Kosterlitz-Thouless transition [35, 36, 37]. For $\mu(T) > 2$, phase slips are confined into neutral pairs, and superconductivity (in the 1D sense of quasi-long-range order) survives the phase fluctuations governed by Eq. (7). However, for $\mu(T) < 2$, phase slips proliferate, the phase stiffness is renormalized to zero, and the system is driven to a normal phase. The true transition temperature then follows from the condition $\mu(T_c) = 2$, which gives

$$\frac{T_c}{T_c^0} = \left[1 - \frac{2}{\nu N} \right]^{2g/(g-1)}. \tag{9}$$

Equation (9) implies that QPSs can lead to a sizeable depression of the mean-field critical temperature for $N < 100$. In Ref. [21] the relative contribution of thermally activated and quantum phase slips has been estimated. Using results from Ref. [36] it has been shown that the crossover temperature between the two regimes is of the order of T_c^0, which implies that for $T < T_c$, with $T_c < T_c^0$, only QPSs significantly affect the resistance below T_c. Indeed, even in the superconducting phase with $\mu > 2$, QPS fluctuations produce a sizeable resistance. Under a small constant current bias, this resistance can be computed from the voltage drop V associated to the occurrence of phase slips via the Josephson relation, see also Ref. [35]. The final result for the linear resistance $R(T < T_c)$ for arbitrary (but larger than ξ) rope length L and thermal length $L_T = \hbar c_s/\pi k_B T$ is [21]

$$\frac{R}{R_Q} = \left(\frac{\pi y \Gamma(\mu/2)}{\Gamma(\mu/2+1/2)}\right)^2 \frac{\pi L}{2\kappa} \left(\frac{L_T}{\kappa}\right)^{3-2\mu} \int_0^\infty du \frac{2/\pi}{1+u^2} \left|\frac{\Gamma(\mu/2 + iuL_T/2L)}{\Gamma(\mu/2)}\right|^4, \qquad (10)$$

where R_Q is the resistance quantum, see Eq. (1), $\Gamma(x)$ denotes the Gamma function, and y and κ are the QPS fugacity and core size, respectively. Equation (10) has been obtained from perturbation theory in the fugacity y, and thus only holds for a dilute QPS gas. This assumption breaks down in the vicinity of T_c, where QPSs proliferate and cause the Kosterlitz-Thouless transition. Equation (10) is therefore only reliable well below T_c, and cannot be used to describe the resistance saturation around $T = T_c$. For $L/L_T \gg 1$, the u-integral approaches unity, and hence $R \propto T^{2\mu-3}$, while for $L/L_T \ll 1$, dimensional scaling arguments give $R \propto T^{2\mu-2}$ [35]. In Refs. [6, 7] typical lengths were $L \approx 1$ μm, which puts one into the crossover regime $L_T \approx L$. Inspection of Eq. (10) also shows that, as expected, the transition becomes broader and broader when the number of tubes decreases. This is illustrated in Fig. 7, where the theoretical resistance curves are depicted for various values of N, taking $\nu = 1$ and $g = 1.3$.

IV. COMPARISON WITH EXPERIMENTS

In this section we compare the theoretical result (10) for the temperature-dependent resistance below T_c with the experimental data. We focus on samples $R2$ and $R4$, where the resistance has been measured down to quite low temperatures, and a meaningful comparison is possible, see Figs. 8 and 9. In this comparison, it has to be borne in mind that Eq. (10) does not take into account the normal contacts. These cause a contact resistance

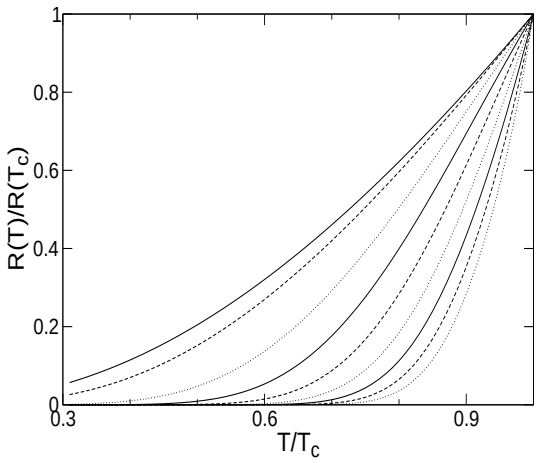

FIG. 7: Temperature-dependent resistance $R(T < T_c)$ predicted by Eq. (10) for $\nu = 1$ and different N. The smaller is N, the broader is the transition. From the leftmost to the rightmost curve, $N = 4, 7, 19, 37, 61, 91, 127, 169, 217$.

(1) which we subtract from the experimental data when comparing to Eq. (10). In addition, the experimentally measured residual resistance fixes the value of N taken in the respective comparison. Moreover, Eq. (10) does not take into account the possible destruction of superconductivity by the normal contacts. Indeed, investigation of the proximity effect at high-transparency NS interfaces has shown that superconductivity resists the presence of normal contacts only if the length of the superconductor is much greater than its coherence length ξ [38]. This is probably the reason why superconductivity is only observed in the longest ropes. Finally, Eq. (10) only applies to temperatures well below T_c, and in particular does not capture quasiparticle effects or phonon backscattering. The transition to the normal-state resistance is not described at this level of theory. Besides N and the LL parameter, which is taken to be $g = 1.3$, another important parameter appearing in the expression for the resistance is the critical temperature T_c. In principle this could be computed once the eigenvalue Λ_1 of the coupling matrix Λ is known. However, as discussed above, to obtain a reliable estimate for Λ_1 is very difficult. In order to circumvent this problem, we remark that it is natural to identify T_c with the experimentally determined transition temperature T^*. Since now both N and T_c are fixed directly by experimental data, there is only one remaining adjustable parameter, namely ν. According to our discussion above, the fit is expected to yield values $\nu \approx 1$.

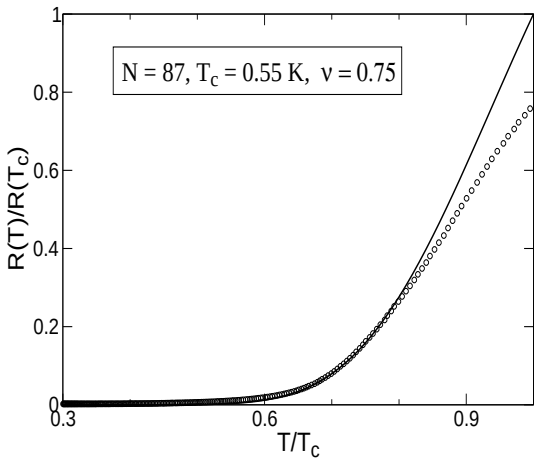

FIG. 8: Temperature dependence of the linear resistance below T_c for sample $R2$. Open circles denote experimental data (with subtracted residual resistance corresponding to $N = 87$), the curve is the theoretical result for $\nu = 0.75$.

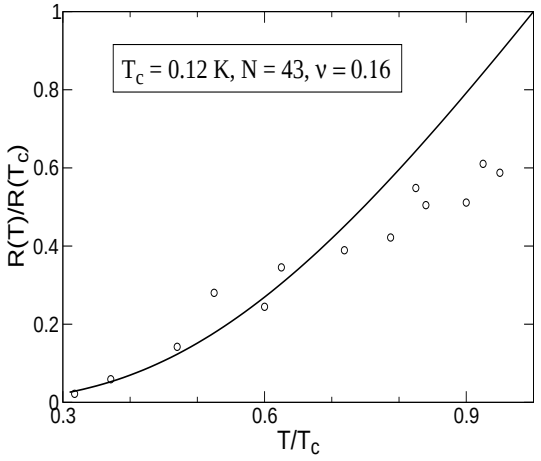

FIG. 9: Same as Fig. 8, but for sample $R4$ with $N = 43$ and $\nu = 0.16$.

In Figs. 8 and 9 the experimental curves are fitted with Eq. (10) using ν as a fit parameter. We obtain as optimal fit values $\nu = 0.75$ for sample $R2$ and $\nu = 0.16$ for sample $R4$, respectively. The first is in very good agreement with the expected theoretical value of ν. For sample $R4$, the optimal ν is smaller than expected, which may indicate that dissipative processes are more important in that sample. It is also possible that the screening of Coulomb interactions is less effective in this narrow rope (where nearly half of the tubes are on the surface) than in the thicker rope $R2$. Nevertheless, for both samples, the low-temperature

resistance agrees quite well, with only one free fit parameter that is found to be of order unity as expected. The theoretical curves clearly do not provide a good description in the vicinity of T_c. This is however the expected consequence of the perturbative nature of our calculation, which breaks down close to T_c due to QPS proliferation. Thus the saturation observed experimentally around $T \approx T^*$ is not captured. Equation (10) also predicts a vanishing linear resistance as $T \to 0$. A finite $T = 0$ resistance is usually expected when, instead of (or in addition to) bound pairs of QPSs, one also considers single QPS events. However, the latter are expected to be important only for short 1D systems and have not been taken into account in our theory. An order-of-magnitude estimate indicates anyway that their contribution to the resistance is exponentially small due to the large $T = 0$ value of μ, and then practically unmeasurable.

We believe that the rather good agreement between the theoretical resistance result (10) and experimental data at low temperatures as shown in Figs. 8 and 9, given the complexity of this system, is rather satisfactory. This comparison provides strong evidence that quantum phase slips have been observed in superconducting nanotube ropes.

Acknowledgments

This work has been supported by the EU network DIENOW. A.K. thanks the Russian foundation for basic research and solid state nanostructures for financial support, and thanks CNRS for a visitor's position. We thank M. Devoret, N. Dupuis, T. Giamarchi, J. González, D. Maslov, and C. Pasquier for stimulating discussions.

---

[1] C. Dekker, Physics Today **52 (5)**, 22 (1999). See also reviews on nanotubes in Phys. World **6**, 1 (2000).

[2] M.S. Dresselhaus, G. Dresselhaus, and P.C. Eklund, *Science of Fullerenes and Carbon Nanotubes* (Academic Press, San Diego, 1996); M.S. Dresselhaus, G. Dresselhaus, and Ph. Avouris (eds.), *Carbon Nanotubes*, Topics in Appl. Physics **80** (Springer, Berlin, 2001).

[3] S. J. Tans, M. H. Devoret, H. J. Dai, A. Thess, R. E. Smalley, L. J. Geerligs, and C. Dekker, Nature **386**, 474 (1997).

[4] A. Yu. Kasumov, R. Deblock, M. Kociak, B. Reulet, H. Bouchiat, I. I. Khodos, Yu. B. Gorbatov, V. T. Volkov, C. Journet, and M. Burghard, Science **284**, 1508 (1999).

[5] A.F. Morpurgo, J. Kong, C.M. Marcus, and H. Dai, Science **286**, 263 (1999).

[6] M. Kociak, A.Yu. Kasumov, S. Gueron, B. Reulet, I.I. Khodos, Yu.B. Gorbatov, V.T. Volkov, L. Vaccarini, and H. Bouchiat, Phys. Rev. Lett. **86**, 2416 (2001).

[7] A. Kasumov, M. Kociak, M. Ferrier, R. Deblock, S. Gueron, B. Reulet, I. Khodos, O. Stephan, and H. Bouchiat, Phys. Rev. B **68**, 214521 (2003).

[8] P.R. Wallace, Phys. Rev. **71**, 622 (1947).

[9] C.T. White and T.N. Todorov, Nature **393**, 240 (1998).

[10] J. M. Luttinger, J. Math. Phys. **4**, 1154 (1963).

[11] A.O. Gogolin, A.A. Nersesyan, and A.M. Tsvelik, *Bosonization and Strongly Correlated Systems* (Cambridge University Press, 1998).

[12] R. Egger and A.O. Gogolin, Phys. Rev. Lett. **79**, 5082 (1997).

[13] C. Kane, L. Balents, and M.P. Fisher, Phys. Rev. Lett **79**, 5086 (1997).

[14] M. Bockrath, D. H. Cobden, J. Lu, A. G. Rinzler, R. E. Smalley, L. Balents, and P. L. McEuen, Nature **397**, 598 (1999).

[15] Z. Yao, H.W.C. Postma, L. Balents, and C. Dekker, Nature **402**, 273 (1999).

[16] H. Ishii *et al.*, Nature **426**, 540 (2003).

[17] B. Gao, A. Komnik, R. Egger, D.C. Glattli, and A. Bachtold, cond-mat/0311645.

[18] H. Grabert and M.H. Devoret (eds.), *Single Charge Tunneling* (Plenum, New-York, 1992).

[19] A.Yu. Kasumov, I.I. Khodos, P.M. Ajayan, and C. Colliex, Europhys. Lett. **34**, 429 (1996); A.Yu. Kasumov *et al.*, Europhys. Lett. **43**, 89 (1998).

[20] A. De Martino and R. Egger, Phys. Rev. B **67**, 235418 (2003).

[21] A. De Martino and R. Egger, preprint (submitted to Phys. Rev. B). For a short version, see cond-mat/0308162.

[22] J. González, Phys. Rev. Lett. **88**, 076403 (2002).

[23] J. González, Phys. Rev. **B 67**, 014528 (2003).

[24] J. González, Eur. Phys. J. B **36**, 317 (2003).

[25] A.A. Maarouf, C.L. Kane, and E.J. Mele, Phys. Rev. B **61**, 11156 (2000).

[26] M. Tinkham, *Introduction to Superconductivity*, 2nd edition (McGraw-Hill, 1996).

[27] N. Giordano, Phys. Rev. **B 50**, 160 (1991).

[28] J. Meyer and G.V. Minnigerode, Phys. Lett. **38A** 529 (1972).

[29] J. Romijn, T.M. Klapwijk, M.J. Renne, and J.E. Mooij, Phys. Rev. B **26**, 3648 (1982).

[30] F. Sharifi, A.V. Herzog, and R.C. Dynes, Phys. Rev. Lett. **71**, 428 (1993); P. Xiong, A.V. Herzog, and R.C. Dynes, Phys. Rev. Lett. **78**, 927 (1997).

[31] C.N. Lau, N. Markovic, M. Bockrath, A. Bezryadin, and M. Tinkham, Phys. Rev. Lett. **87**, 217003 (2001).

[32] R. Egger and A.O. Gogolin, Eur. Phys. J B **3**, 281 (1998).

[33] N. Nagaosa, *Quantum Field Theory in Condensed Matter Physics* (Springer Verlag, 1999).

[34] J.E. Mooij and G. Schön, Phys. Rev. Lett. **55**, 114 (1985).

[35] A.D. Zaikin, D.S. Golubev, A. van Otterlo, and G.T. Zimanyi, Phys. Rev. Lett. **78**, 1552 (1997).

[36] D.S. Golubev and A.D. Zaikin, Phys. Rev. B **64**, 014504 (2001).

[37] P.M. Chaikin and T. Lubensky, *Principles of Condensed Matter Physics* (Cambridge University Press, 2000).

[38] W. Belzig, C. Bruder, and G. Schön, Phys. Rev. B **54**, 9443 (1996).